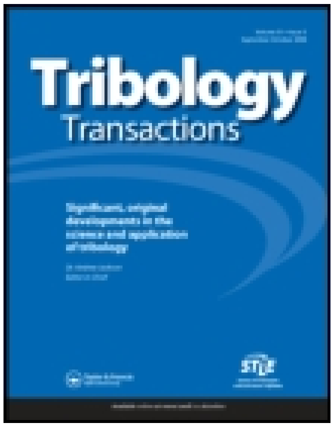

Tribology Transactions
Publication details, including instructions for authors and subscription information:
http://www.tandfonline.com/loi/utrb20

EHL Film Thickness Limitation Theory Under a Limiting Shear Stress

Yongbin Zhang [a] & Shizhu Wen [a]
[a] Tsinghua University, National Tribology Laboratory , Beijing, 100084, P. R. of China
Published online: 25 Mar 2008.

Vol. 45 (2002), 4, 531-539
TRIBOLOGY TRANSACTIONS

EHL Film Thickness Limitation Theory Under a Limiting Shear Stress©

YONGBIN ZHANG and SHIZHU WEN
Tsinghua University
National Tribology Laboratory
Beijing, 100084, P. R. of China

It is numerically shown that the elastohydrodynamic lubrication (EHL) film thickness has a limit under an assumed limiting shear stress of the contact-lubricant interface in isothermal pure rolling line contacts. The prediction of the central film thickness limit is made, and well matches experiments. The present theory shows that, in elastohydrodynamic line contacts, the central film thickness is of molecular scale and part of the contact area is in non-continuum film lubrication when the equivalent cylinder curvature radius is less than the critical one. This critical radius depends on the load and the contact-lubricant interfacial limiting shear stress at low pressures.

Final manuscript approved June 12, 2002
Review led by Steven Danyluk

KEY WORDS

Elastohydrodynamic Lubrication; Film Thickness Limit; Interfacial Limiting Shear Stress

NOMENCLATURE

C	= dimensionless ambient interfacial limiting shear stress, $\tau_{l0}/(E'G^{0.4})$
C_p	= $\tau_{l0}/(kE'G^{0.4})$
E_1, E_2	= Young's elasticity moduli of the cylinder and plane surfaces, respectively
E'	= equivalent Young's elasticity modulus, $1/E' = 1/2[1-\nu_1^2)/E_1 + (1-\nu_2^2)/E_2]$
$f_0(\tau), f_1(\tau)$	= functions, Eqs.[3] and [4]
G	= material parameter, $\alpha E'$
G_∞	= shear elasticity modulus
h_c	= central film thickness
$h_{c,\max}$	= central film thickness limit
$H_{c\max}$	= dimensionless central film thickness limit, $h_{c,\max}/R$, Eq.[19]
k	= τ_{l0}/τ_{l0cp}
K, n and U_{b0}	= variables dependent on C, Eqs.[13]-[15]
K_1, n_1 and U_{b1}	= variables having the values of K, n and U_{b0} respectively when C_p is substituted for C
p	= film pressure
p_h	= maximum Hertzian pressure, $\sqrt{wE'/(2\pi R)}$
p_s	= lubricant solidification pressure
r_{it}, m_w	= variables dependent on G, U and W, Tables 3 and 4
R	= equivalent cylinder curvature radius
R_{cr0}	= critical equivalent cylinder curvature radius less than which for the equivalent cylinder curvature radius, the non-continuum film is generated in line contact EHL
t	= time
T	= lubricant temperature
u	= rolling speed
u_b	= the rolling speed which makes the interfacial slippage start to occur in the inlet zone
u_d	= the rolling speed beyond which the central film thickness remains constant
u_p	= the rolling speed which is used for prediction of the central film thickness limit
U	= operational parameter, $\eta_0 u/(E'R)$
U_b	= dimensionless form of $u_b, \eta_0 u_b/(E'R)$, Eq. [11]
U_p	= dimensionless form of $u_p, \eta_0 u_p/(E'R)$, Eq.[18]
w	= load per unit axial length
W	= operational parameter, $w/(E'R)$
x	= coordinate
ν_1, ν_2	= Poisson's ratios of the cylinder and plane surfaces, respectively
α	= lubricant viscosity-pressure index
$\alpha_{\tau l}$	= interfacial limiting shear stress-pressure proportionality
τ	= shear stress
τ_b	= shear stress at the contact-lubricant interface
τ_{l0}	= ambient interfacial limiting shear stress
τ_l	= interfacial limiting shear stress
τ_{l0c}	= required or critical ambient interfacial limiting shear stress which prevents the interfacial slippage in the inlet zone
τ_{l0cp}	= critical ambient interfacial limiting shear stress for the speed of U_p, Eq. [17]
η	= lubricant viscosity
η_0	= lubricant viscosity at ambient pressure
ρ_0	= lubricant density at ambient pressure
$\dot\gamma$	= shear strain rate
Δu	= film slipping velocity at the contact-lubricant interface, which is the film speed at the interface minus the contact surface speed

INTRODUCTION

Conventional EHL theories are challenged by recently established interfacial limiting shear stress and slip EHL theories. Zhang and Wen (2002a) analyzed EHL of line contacts incorporating the contact-lubricant interfacial limiting shear stress, and found EHL film collapse and failure at large slide-roll ratios in the condition of heavy loads. In an earlier study, Wen and Zhang (2000) predicted an inlet zone slip and much reduced film thickness compared to conventional EHL theory for pure rolling, and found the same phenomena of EHL film for large slide-roll ratios and heavy loads when using a lower interfacial limiting shear stress. Their results are new for explaining experimentally observed EHL film collapse and failure (Lee et al., 1973; Czichos, 1974), which is not explained by conventional EHL theories.

Ehret et al. (1998) established an interfacial slip EHL theory for explaining the dimples of sliding EHL contacts experimentally observed by Kaneta et al. (1992). Their theory was capable of explaining Kaneta's interferograms. However, there are several questionable results in their theory. One is that the film thickness increased with slip, which showed that slip increases the load-carrying capacity of EHL films. This result is contradictory to that of Zhang and Wen (2002a, 2002b), which showed that interfacial slip leads to EHL film loss. This result may also be contradictory to that of Rozeanu (1980). His results showed that interfacial slip reduces the load-carrying capacity of hydrodynamic lubrication films. The second questionable result in their theory is that the film pressure increased with slip. However, both the results of Zhang and Wen (2002a) and Rozeanu (1980) showed that film pressure decreases with increasing interfacial slip in EHL and hydrodynamic sliding bearings. The reason for these questionable results may be that Ehret et al. described interfacial slip with over assumptions but both Zhang and Wen (2002a) and Rozeanu (1980) showed substantial physical insights into interfacial slip with reasonable assumptions. The third problem of Ehret's theory is that it may be unable to explain film collapse and failure at heavy loads in Kaneta's experiment (1992) for the full speed range, which should occur according to Czichos (1974).

Kaneta et al. (1996) raised their observed dimples at medium loads of sliding EHL point contacts challenging conventional theories. First, the lubrication in their experiment easily deviates from conventional EHL theories, since their experiment is where film collapse and failure easily occurs at modest loads (Lee et al., 1973; Czichos, 1974). Secondly, they showed abnormal interferograms of their experimental contacts compared with conventional ones, but were not aware that their observed phenomena may be the same with the earlier findings by Lee et al. (1973) for the similar case, which showed anomalous results of film thickness and its variation with load in their experiment compared with conventional EHL theories indicating severe film collapse at relatively heavy loads. Surprisingly, Kaneta et al. (1996) measured the film thickness higher than conventional EHL theory prediction indicating dimples of their contacts. Their measurement should be rather abnormal, since simple sliding normally results in reduced film thickness compared with conventional EHL theories as measured by Lee et al. (1973). As the present authors understand, the measurement of EHL film thickness from interferograms is not accurate because of error judgment of interferometric orders. Despite this, they later found that thermal Newtonian theory can explain their phenomena (Yang et al., 2001). As with Ehret's theory (1998), their theory showed that simple sliding increases the load-carrying capacity of EHL films. The present authors seriously wonder whether their theory is applicable to the case of heavy loads where severe film collapse occurs. Compared with others' similar experiments (Lee et al., 1973; Czichos, 1974), Kaneta's experimental results (1996) appear too particular. The reason for this may need to be examined. The second problem of their theory (Yang et al., 2001) is that it may be unable to explain the irreversibility of "dimples" with sliding speed observed by Kaneta et al. (1996). It is possible that the combined effect of interfacial slip and oil film viscous heating generates the observed phenomena of friction coefficient, abrupt interferogram pattern formation and disappearance, and the irreversibility of interferograms with sliding speed in Kaneta's experiments (1996), since this effect can cause these phenomena because of the irreversible interfacial shear stress, interfacial limiting shear stress and then interfacial slip with sliding speed due to oil film viscous heating. However, this effect usually results in lower film thickness than conventional EHL theory prediction. It seems necessary to further justify Kaneta's experiments from the measured film thickness and with the theories incorporating this effect.

In theory and practice, most challenging to conventional EHL theories is the film collapse and failure in real EHL contacts in the condition of high speed, heavy load and high bulk lubricant temperature. It was suggested by Rozeanu (1980) that the bonding strength between the contact-adhering layer and the bulk lubricant may be rather limited and the interfacial slippage may be present and reduce the film load-carrying capacity in hydrodynamic lubrications. Zhang and Wen (2002a) showed that the contact-lubricant interfacial slippage is convincing in interpreting elastohydrodynamic film collapse and failure based on conventional interfacial limiting shear stress predictions. Czichos and Kirschke (1972) proposed that the endurable contact-lubricant interfacial stresses can only be low in EHL for high contact surface temperatures.

The EHL film collapse and failure in the condition of high bulk lubricant temperatures was found not to be explained by conventional EHL theories and attributed to the thermal desorption of the lubricant from contact surfaces (Czichos, 1974). In this condition, the contact-lubricant interfacial limiting shear stress may be significantly low. For this case, the interfacial slippage may largely reduce the load-carrying capacity of EHL films.

The conventional interfacial limiting shear stress prediction, which extrapolates for low pressures from high pressures, was suspected to overestimate the interfacial limiting shear stress in EHL inlet zones (Zhang and Wen, 2000). This prediction is questionable especially for the case of high contact surface temperatures because it lacks experimental data support.

For high contact surface temperatures, the contact-lubricant interfacial limiting shear stress may better fit the following equations:

$$\tau_l = \begin{cases} \tau_{l0} & \text{for } p < p_s \\ \tau_{l0} + \alpha_{\tau l}(p - p_s) & \text{for } p \geq p_s \end{cases} \quad [1]$$

Table 1—The Lubricant Property Data

Lubricant Density, ρ_0	892kg/m^3 (40°C, 100°C)
Ambient Lubricant Viscosity, η_0	0.106 Pa• s (40°C) 0.012 Pa•s (100°C)
Lubricant Viscosity-Pressure Index, α	21.9GPa^{-1} (40°C) 15.4GPa^{-1} (100°C)
Lubricant Solidification Pressure, p_s	0.82GPa (40°C), 1.77GPa (100°C)

Table 2—Operating Parameters

Cylinder Radius, R	20 mm
Elastic Modulus, E_1, E_2	193.0 GPa
Poisson's Ratio, ν_1, ν_2	0.28
Ambient Interfacial Limiting Shear Stress, τ_{l0}	1.0MPa (40°C) 0.5MPa (100°C)
Limiting Shear Stress-Pressure Proportionality, $\alpha_{\tau l}$	0.030 (40°C) 0.028 (100°C)

Equation [1] was proposed by Zhang and Wen (2000) to be probably better and gives lower values than the conventional interfacial limiting shear stress prediction.

Considering interfacial slippage and utilizing Eq.[1], the present study explores elastohydrodynamic lubrication of line contacts in isothermal and pure rolling conditions with high bulk lubricant temperatures. The purpose of the present study is to examine the load-carrying capacity of EHL films when the contact-lubricant interfacial limiting shear stress and interfacial slippage is taken into account. This is of particular interest to the investigation of EHL film collapse and failure.

LIMITING SHEAR STRESS

Johnson and Tevaarwerk (1977) proposed by experiment that when EHL fluid is strongly solidified, it should have a shear strength. A fluid shear strength as a fundamental fluid property, has been experimentally identified (Paul and Cameron, 1979). It is the highest shear stress that the fluid can withstand.

In severely heated elastohydrodynamic contacts as experimentally examined by Czichos and Kirschke (1972), the physical and chemical reactions at the contact-lubricant interface weakens the fluid adherence to the contact surface and the endurable interfacial stresses become low. Rozeanu and Snarsky (1978) showed that due to entropy repulsion, the bonding strength between the contact surface-adhering layer and the bulk lubricant is lower than those between the molecules in the bulk lubricant and between the molecules in the adhering layer. This means that there is a maximum endurable shear stress of the interface and this stress can be smaller than the fluid shear strength.

In isothermal EHL films, the operating limiting shear stress is at the contact-lubricant interface instead of inside the film (Zhang and Wen, 2002a). This stress limits the shear stress of the EHL film. The interfacial limiting shear stress is therefore the maximum endurable shear stress of the interface or the fluid shear strength, whichever is less.

In the present study, the interfacial limiting shear stress is not critically distinguished as the fluid shear strength or the maximum endurable shear stress of the interface, and is the minimum of them. However, both the fluid shear strength and the maximum endurable shear stress of the interface has not been finely understood. Formulating them seems still a difficulty at present. In the present study, the values of the interfacial limiting shear stress are chosen and predicted from some experiments on fluid shear strength.

At high contact surface temperatures, the physical and chemical reactions between the lubricant and the contact surface reduces the interfacial shear strength to low values (Czichos, 1974; Bailey and Cameron, 1973). Due to this fact, relatively low values of the limiting shear stress such as below 1MPa are taken in the present study. These values may be correct in an EHL contact, however may be unobservable in a usual viscometer because of different interfacial conditions. Here, the interfacial limiting shear stress is assumed to follow Eq. [1].

ANALYSIS

Zhang and Wen (2002a) derived an analysis for EHL, which directly showed the relation between interfacial slip and interfacial limiting shear stress. Interfacial slip is a result of interfacial shear stress exceeding interfacial limiting shear stress. Since interfacial limiting shear stress physically exists, interfacial slip in EHL is physically existent. Although Ehret et al. (1998) considered interfacial slip in EHL, they failed to describe the dependence of interfacial slip on interfacial limiting shear stress. This makes the validity of their analysis heavily questionable.

The present study adopted Zhang and Wen's analysis (2002a). This analysis is numerical and based on the following fluid model:

$$\tau = \begin{cases} \eta\dot{\gamma} & \text{for} |\tau| < \tau_l \\ sign(\dot{\gamma})\tau_l & \text{for } |\tau| \geq \tau_l \end{cases} \qquad [2]$$

where τ_l is the interfacial limiting shear stress.

In the present study, the contacts are formed by a cylinder and a plane, and are ideally smooth. The flow is one dimensional. The condition is isothermal, steady-state and pure rolling.

PARAMETERS

In the present analysis, the rolling speed varies from 0.02m/s to 10.0m/s, and the load varies from 150N/mm to 12000N/mm corresponding to the maximum Hertzian pressures from 0.5 GPa to 4.47GPa. The lubricant is a paraffinic mineral oil. The lubricant property data are shown in Table 1.

The operating parameters are listed in Table 2.

FILM THICKNESS RESULTS

The present results show that for low rolling speeds (less than 0.1m/s), there is no interfacial slippage in the inlet zone and the central film thickness is the same as based on the Newtonian fluid model. When the lubricant temperature T is 40°C and the load is 300N/mm (which gives the maximum Hertzian pressure p_h 0.71GPa), for the rolling speed 0.4m/s, there is no appreciable interfacial slippage in the inlet zone but the subsequent rolling speed increase generates interfacial slippage rapidly. This is shown in Fig. 1. The interfacial slippage is found from the interfacial slipping velocity Δu, which is the film speed at the interface

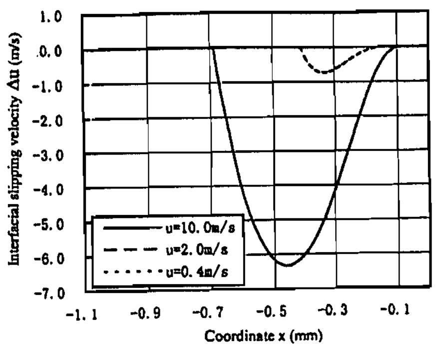

Fig. 1—The slipping velocity at both the cylinder-lubricant and plane-lubricant interfaces in the inlet zone for different rolling speeds. The Hertzian zone is from -0.27mm to 0.27mm, p_h =0.71GPa, T=40°C.

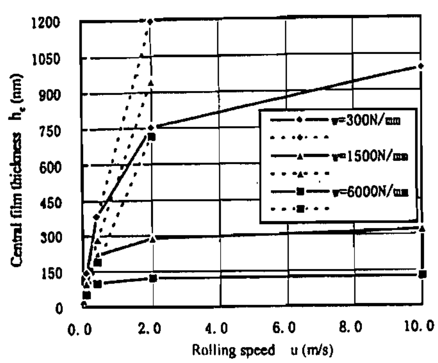

Fig. 2—The central film thickness-speed relations under different loads, T=40°C. Solid line denotes the results based on the present model and dashed line denotes the results based on the Newtonian fluid model.

minus the contact surface speed. The interfacial slipping velocity shows the slippage region Δu = 0 represents no interfacial slippage.

Figure 1 shows that the rolling speed increase rapidly enlarges the extent and magnitude of the interfacial slippage and results in the interfacial shear stress in a much increased region (where the interfacial slippage occurs) reduced by the interfacial limiting shear stress. This reduces the film thickening effect of the rolling speed increase.

Figure 2 shows the central film thickness-speed relations for different loads. For the load 300N/mm or p_h = 0.71GPa, for the rolling speed over 0.4m/s, the central film thickness-speed relation based on the present model deviates from that based on the Newtonian fluid model. For the load 1500N/mm or p_h = 1.57GPa, the central film thickness is insensitive to the variation of the rolling speeds over 2.0m/s. For the load 6000N/mm or p_h = 3.16GPa, the central film thickness for the rolling speeds over 2.0m/s is nearly constant. Figure 2 indicates that the interfacial limiting shear stress effect limits EHL film thickness.

For T=40°C, u=10.0m/s and τ_{l0}=1.0MPa, the present results show that the central film thickness for the load 1500N/mm is 105nm and that for the load 2500N/mm is 77nm. For T=100°C, which gives τ_{l0} 0.5MPa, and u=10.0m/s, the central film thickness for the load 1500N/mm is 98nm and that for the load 2500N/mm is 70nm. Note that for these heavy loads, the rolling speed 10.0m/s gives central film thickness nearly independent of the rolling speed. The comparisons of the above data shows that the central film thickness limit is independent of lubricant viscosity but related to the ambient interfacial limiting shear stress .

It is clear that the present film thickness limit results from the reduction of the shear stress at the contact-lubricant interface by the limiting shear stress (Zhang and Wen, 2002a). For a fixed load, in the EHL inlet zone, since the film thickness rapidly increases with rolling speed but the film pressure gradient has a relatively weak sensitivity to rolling speed, according to the relation, $\partial p/\partial x = 2\tau_b/h$, increasing rolling speed makes the shear stress at the interface in the inlet zone increase rapidly because of the film pressure gradient and the film thickness. When the limiting shear stress at the interface is low so that a modest rolling speed makes the interfacial shear stress exceed the interfacial limiting shear stress in the inlet zone and consequently makes the interfacial slippage occur there, the interfacial slippage region is rapidly enlarged by a further rolling speed increase as shown by Fig. 1. Hence it is expected that, when the rolling speed is sufficiently high, the effective interfacial shear stress for building the film pressure gradient and the film thickness in the inlet zone, which is close to the Hertzian zone and is the interfacial limiting shear stress, should become not varied with rolling speed, the film pressure gradient in the inlet zone has a very weak sensitivity to rolling speed, and therefore the film thickness remains constant in the inlet zone and consequently in the Hertzian zone in spite of further rolling speed increases. This film thickness is considered as the film thickness limit. Figures 3 and 4 shows the rolling speed influence on the film pressure profile and the interfacial shear stress in the inlet zone. Figure 5 shows the film thickness distributions for different rolling speeds.

THE BOUNDARY IN LINE CONTACT EHL BETWEEN THE VISCOELASTIC-LUBRICANT AND VISCOPLASTIC-LUBRICANT REGIMES

Conventional EHL theories do not consider the contact-lubricant interfacial limiting shear stress. Its lubricant rheological model is commonly written as :

$$\dot{\gamma} = \frac{1}{G_\infty}\frac{d\tau}{dt} + \frac{1}{\eta}f_0(\tau) \qquad [3]$$

Equation [3] represents a viscous and elastic lubricant. However, Eq. [3] does not fit the lubricant behavior at high shear rates. This behavior exhibits a 'solid-like' plastic flow due to the interfacial limiting shear stress. Hence, the lubricant rheological model for EHL should be better written as :

$$\dot{\gamma} = \frac{1}{G_\infty}\frac{d\tau}{dt} + \frac{1}{\eta}f_1(\tau,\tau_l) \qquad [4]$$

where τ_l is the interfacial limiting shear stress. Eq.[4] represents a viscoplastic and elastic lubricant. When τ_l tends to infinity, Eq. [4] reduces to Eq. [3].

In elastohydrodynamic lubrication, it was shown by Zhang and Wen (1998) that when the ambient interfacial limiting shear stress τ_{l0} exceeds the critical interfacial limiting shear stress τ_{l0c}, no interfacial slippage occurs in the inlet zone and Eq. [3] is valid for film thickness calculation, while when $\tau_{l0} < \tau_{l0c}$, interfacial slippage occurs in the inlet zone, Eq. [4] must be utilized for film

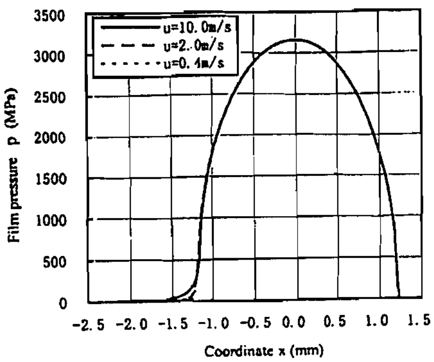

Fig. 3—The rolling speed influence on film pressure profile. p_h = 3.16 GPa, T=40°C.

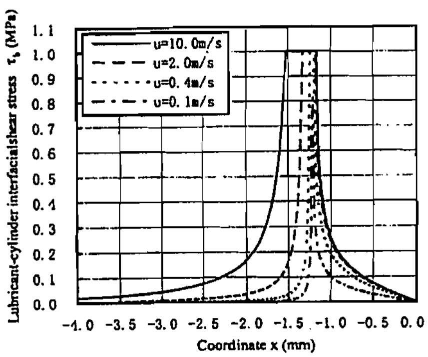

Fig. 4—The rolling speed influence on the cylinder-lubricant interfacial shear stress in the inlet zone. p_h = 3.16 GPa, T=40°C.

thickness calculation, and the resulting film thickness is lower than conventional theory predicts. It is therefore clear that at least two lubrication regimes i.e. the viscoelastic-lubricant regime and the viscoplastic-lubricant regime play in two separate elastohydrodynamic lubrication operational regions and the transition between these two regimes occurs on certain operating points when the interfacial limiting shear stress is considered. When EHL is in the viscoelastic-lubricant regime, conventional EHL film thickness prediction is valid, while when EHL is in the viscoplastic-lubricant regime, the EHL film thickness should be based on the lubricant rheological model which incorporates the interfacial limiting shear stress.

The discussion above shows that only when the rolling speed exceeds a critical value u_b, the central film thickness deviates from that based on the Newtonian fluid model. EHL film thickness is determined by the lubricant rheological behavior in the inlet zone. This behavior is Newtonian according to the present model unless there is a location in the inlet zone where the interfacial shear stress reaches the interfacial limiting shear stress or the interfacial slippage occurs (Zhang and Wen, 2002a). u_b can be considered as the rolling speed which makes the interfacial shear stress in the inlet zone start to reach the interfacial limiting shear stress and therefore makes the interfacial slippage start to occur there. For the present case, the required or critical ambient interfacial limiting shear stress which prevents the interfacial slippage in the inlet zone is (Zhang and Wen,1998) :

$$\tau_{l0c} = \frac{11.9}{8.0} E' r_{it}(1 - r_{it}^2)^{-0.5} G^{0.4} U^{0.74} W^{-0.2} \quad [5]$$

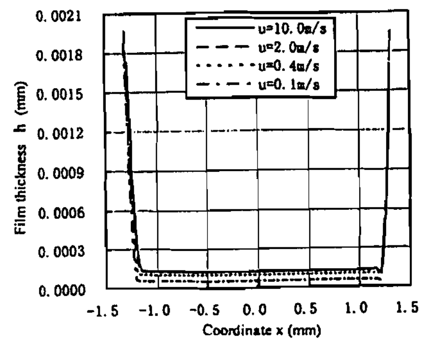

Fig. 5—The film thickness distributions for different rolling speeds. p_h = 3.16 GPa, T=40°C.

where, E' is the equivalent contact modulus of elasticity, $G = \alpha E'$, $W = w/(E'R)$, $U = \eta_0 u/(E'R)$, and r_{it} is a parameter dependent on G, U and W. To give a more precise prediction for τ_{l0c}, Eq. [5] is corrected as :

$$\tau_{l0c} = \frac{11.9}{8.0} m_w E' r_{it}(1 - r_{it}^2)^{-0.5} G^{0.4} U^{0.74} W^{-0.2} \quad [6]$$

where m_w reduces the prediction error, which is caused by the numerical values of r_{it} and the equation prediction of the central film thickness (see Zhang and Wen, 1998), and is written as :

$$m_w = m_w(G, U, W) \quad [7]$$

For the ambient interfacial limiting shear stress τ_{l0}, the non-dimensional form (U_b) of u_b satisfies:

$$\tau_{l0} = \frac{11.9}{8.0} m_w E' r_{it}(1 - r_{it}^2)^{-0.5} G^{0.4} U_b^{0.74} W^{-0.2} \quad [8]$$

Define:

$$C = \frac{\tau_{l0}}{E' G^{0.4}} \quad [9]$$

and rewrite Eq. [8] as :

$$C = \frac{11.9}{8.0} m_w r_{it}(1 - r_{it}^2)^{-0.5} U_b^{0.74} W^{-0.2} \quad [10]$$

Solving the coupled equations of $r_{it} = r_{it}(G, U, W)$, Eq. [7] and Eq. [10] for U_b gives :

$$U_b = f(G, W, C) \quad [11]$$

For the typical case G=4500, r_{it} and m_w is shown in Tables 3 and 4, respectively. $m_w(G,U,W)$ and $r_{it}(G,U,W)$ are obtained from numerical computation. The untabulated values of m_w and r_{it} can be interpolated or extrapolated from their available values.

For E'= 209GPa, G = 4500 and τ_{l0} =0.0 to 20.0MPa, C is between 0.0 and 3.302×10^{-6}. For G=4500, the solution of U_b is:

$$U_b = U_{b0} + \frac{K}{W^n} \quad [12]$$

where U_{b0}, K and n are regressed out as :

TABLE 3-THE VALUES of r_u (G=4500)

U \ r_u \ W	4.77 e-6	1.07 e-5	1.79 e-5	2.74 e-5	3.58 e-5	5.37 e-5	7.16 e-5	1.07 e-4	1.43 e-4	2.15 e-4	3.58 e-4	5.97e -4	9.55 e-4	1.43 e-3	2.15 e-3	2.87 e-3
2.53e-10					0.712	0.767	0.800	0.819	0.870	0.900	0.950	0.970	0.980	0.984	0.990	0.993
1.77e-10					0.724	0.773	0.802	0.843	0.879	0.915	0.952	0.972	0.983	0.986	0.991	0.994
1.01e-10					0.738	0.792	0.815	0.856	0.886	0.921	0.954	0.976	0.984	0.989	0.992	0.9945
5.06e-11					0.763	0.806	0.875	0.886	0.921	0.945	0.955	0.978	0.987	0.990	0.993	0.995
4.05e-11				0.753	0.775	0.817	0.884	0.898	0.930	0.950	0.967	0.979	0.988	0.991	0.9935	0.9955
2.02e-11				0.780	0.806	0.852	0.893	0.909	0.932	0.954	0.972	0.983	0.989	0.993	0.995	0.996
1.01e-11			0.736	0.792	0.838	0.887	0.910	0.931	0.955	0.966	0.978	0.985	0.990	0.993	0.995	0.996
6.33e-12			0.811	0.829	0.852	0.904	0.921	0.943	0.960	0.972	0.984	0.990	0.994	0.995	0.995	0.996
2.53e-12		0.808	0.856	0.887	0.898	0.920	0.930	0.955	0.966	0.980	0.990	0.992	0.995	0.995	0.996	0.997
1.27e-12		0.869	0.886	0.910	0.932	0.946	0.955	0.967	0.979	0.988	0.992	0.9945	0.9955	0.9967	\	\
5.06e-13	0.839	.0.908	0.931	0.944	0.955	0.967	0.977	0.979	0.990	0.992	0.995	0.997	\	\	\	\

TABLE 4 -THE VALUES of m_w (G=4500)

U \ m_w \ W	4.77 e-6	1.07 e-5	1.79 e-5	2.74 e-5	3.58 e-5	5.37 e-5	7.16 e-5	1.07 e-4	1.43 e-4	2.15 e-4	3.58 e-4	5.97 e-4	9.55 e-4	1.43 e-3	2.15 e-3	2.87 e-3
2.53e-10					0.536	0.659	0.731	0.907	0.868	0.942	0.875	0.864	0.880	0.944	0.863	0.813
1.77e-10					0.599	0.730	0.813	0.915	0.934	0.966	0.926	0.903	0.870	0.944	0.867	0.827
1.01e-10					0.730	0.828	0.918	1.019	1.052	1.072	1.040	0.948	0.948	0.947	0.884	0.776
5.06e-11					0.857	0.968	0.852	1.069	1.006	0.943	1.203	1.046	0.847	0.955	0.849	0.857
4.05e-11				0.795	0.888	0.995	0.900	1.059	1.018	1.032	1.060	1.078	0.971	1.027	0.873	0.839
2.02e-11				0.887	0.975	1.061	1.026	1.176	1.166	1.134	1.097	1.086	1.107	1.000	0.971	0.857
1.01e-11			0.954	1.070	1.075	1.081	1.100	1.180	1.063	1.110	1.123	1.176	1.152	0.924	0.961	0.679
6.33e-12			0.876	1.070	1.150	1.114	1.146	1.177	1.125	1.121	1.046	1.020	0.962	0.983	0.907	0.680
2.53e-12		0.870	0.958	1.080	1.184	1.244	1.366	1.281	1.264	1.172	1.024	1.160	0.990	0.888	0.813	0.802
1.27e-12		0.852	1.063	1.115	1.103	1.200	1.242	1.268	1.122	0.986	0.964	0.950	0.872	0.738	\	\
5.06e-13	0.831	.0.875	1.008	1.092	1.111	1.150	1.043	1.256	0.903	0.992	1.110	\	\	\	\	\

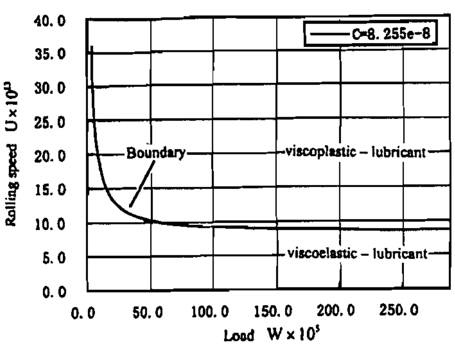

Fig. 6(a)—The boundary between the viscoelastic-lubricant and viscoplastic-lubricant regimes, G=4500.

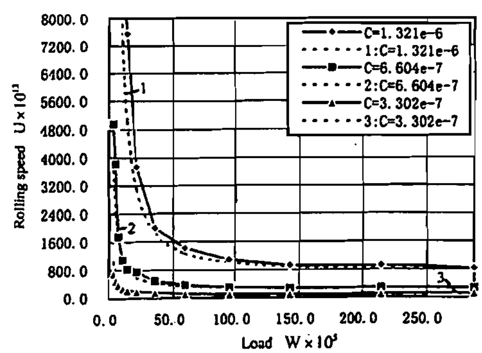

Fig. 6(b)—The boundary between the viscoelastic-lubricant and viscoplastic-lubricant regimes, G=4500. Solid line denotes the precise boundary (resulting from Eq. [11]) and dashed line denotes the predicted boundary from Eq. [12].

$$U_{b0} = 27.8249C^2 + 2.115843 \times 10^{-5}C - 1.11009 \times 10^{-12} \quad [13]$$

$$K = 5.46235 \times 10^{-10}C + 5.391 \times 10^{-17} \quad [14]$$

$$n = 1.02806\text{x}10^{18}\, C^3 - 2.4495\text{x}10^{12}\, C^2 + 1.91326\text{x}10^6\, C + 0.8582 \quad \text{for } C \le 3.302\text{x}10^{-7}$$

$$n = 2.347\text{x}10^5\, C + 1.1825 \quad \text{for } C > 3.302\text{ x }10^{-7} \quad [15]$$

The comparison shows that Eq. [12] is comparatively precise at least when $W = 1.0\text{x}10^{-6}$ to $1.0\text{x}10^{-2}$, $U = 1.0\text{x}10^{-13}$ to $1.0\text{x}10^{-9}$ and $C = 8.255\text{x}10^{-8}$ to $1.981\text{x}10^{-6}$. This operational scope usually corresponds to τ_{l0} from 0.5MPa to 12.0MPa. The boundary between the viscoelastic-lubricant and viscoplastic-lubricant regimes predicted by Eq. [12] is shown typically in Fig. 6(a). Figure 6(b) describes the boundaries for various C and compares the precise and predicted boundaries.

PREDICTION OF THE CENTRAL FILM THICKNESS LIMIT

The film thickness results section showed that when the rolling speed exceeds a certain value u_d, the central film thickness

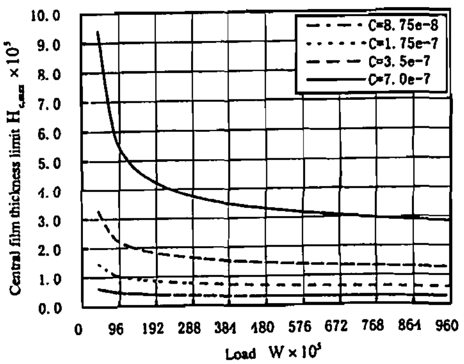

Fig. 7—The central film thickness limit against load, G=4500.

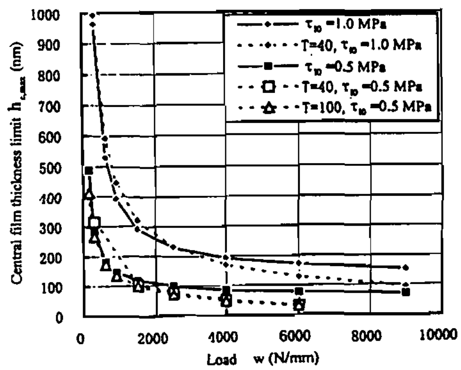

Fig. 8(a)—Comparison between the prediction of the central film thickness limit and the numerical results. Solid line denotes the prediction from Eq. [19] and dashed line denotes the numerical results.

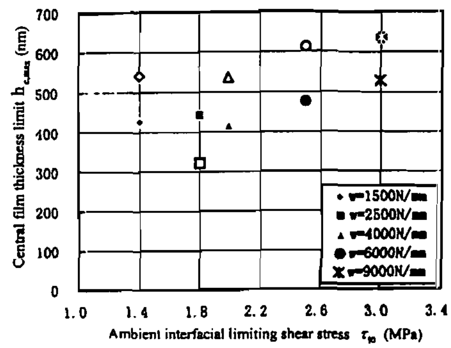

Fig. 8(b)—Comparison between the prediction of the central film thickness limit and the numerical results. Solid mark denotes the prediction from Eq. [19] and empty mark denotes the numerical results.

remains constant and the central film thickness for u_d is considered as the central film thickness limit. It seems exacting to derive the central film thickness limit with u_d. A simple method is to assume the central film thickness for U_p predicted from conventional EHL theory (Wen, 1990) as the central film thickness limit. According to this, the central film thickness limit is:

$$H_{c,max} = 11.9G^{0.4}U_p^{0.74}W^{-0.2} \qquad [16]$$

Assume the critical ambient interfacial limiting shear stress for U_p is τ_{l0cp}, i.e.:

$$\tau_{l0cp} = \frac{11.9}{8.0}m_w E' r_{it}(1 - r_{it}^2)^{-0.5}G^{0.4}U_p^{0.74}W^{-0.2} \qquad [17]$$

Define $k = \tau_{l0}/\tau_{l0cp}$; Eq. [11] gives :

$$U_p = f(G, W, C_p) \qquad [18]$$

where $C_p = \tau_{l0}/(kE'G^{0.4})$ and k depends on G, U and W. For G=4500, the numerical results show that k has the value 0.53. Hence, for this case the central film thickness limit is:

$$H_{c,max}(W, C_p) = 344.2(U_{b1} + \frac{K_1}{W^{n_i}})^{0.74}W^{-0.2} \qquad [19]$$

where, $Cp = 1.887C = 0.0652\tau_{l0}/E'$, U_{b1}, K_1 and n_1 have the values of U_{b0}, K and n respectively when substituting C_p for C.

Figure 7 plots the central film thickness limit against load for various C. Figure 7 shows that the parameter C has a decisive effect on the central film thickness limit; the central film thickness limit is sensitive to the variation of load in the light load range but insensitive to that in the heavy load range. Figures 8(a) and 8(b) compares the prediction from Eq. [19] with the numerical results. Since the lubricant temperatures (T) 40°C and 100°C respectively give G=4500 and G=3200, Fig. 8(a) shows that the lubricant temperature and therefore G has a weak influence on the central film thickness limit for a given τ_{l0}.

The central film thickness limit usually occurs under high rolling speeds. This condition commonly generates remarkable lubricant film viscous heating. Equation [16] shows that the central film thickness limit is determined by G, W and U_p and is independent of fluid viscosity. The interpretation for this is that the central film thickness limit will occur under higher rolling speeds when the fluid viscosity is lower but its magnitude remains constant. Hence, the temperature effect on the present film thickness limit is caused by the strong influence of temperature on the interfacial limiting shear stress. These are shown in the film thickness results section and Fig. 8(a).

COMPARISON WITH EXPERIMENTS

Experimental film thickness results were presented by Kannel and Bell (1971) with a paraffinic mineral oil and a polyphenyl ether (5P4E oil). The film thickness was measured under the rolling speed 46.23m/s /9100fpm. Their measured film thickness was shown not to be explained by conventional EHL theories, but examined by themselves to be correct. Kannel and Bell's film thickness measurement with the X-ray technique may be less accurate compared to the lubricant film thickness measurement with optical interferometry technique. Currently, the optical interferometry technique is more adopted in lubricant film thickness measurement because of its higher precision. In spite of this, Kannel and Bell's film thickness measured with X-ray technique can be compared with the present results.

Kannel and Bell's measured film thickness very slightly varies with the rolling speed when the rolling speed is over 34.54m/s/6800fpm. This is unable to be explained by conventional isothermal and thermal EHL theories. No theories were found to well match them. These film thicknesses may be the film thickness limit. The present theory is compared with these film thick-

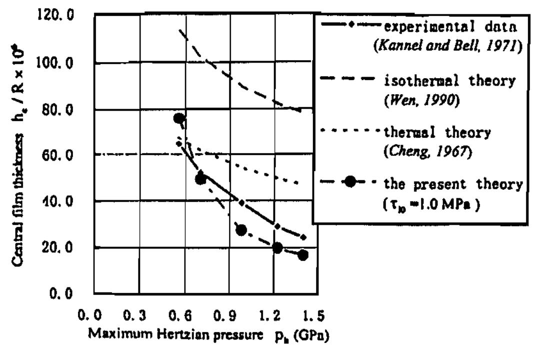

Fig. 9(a)—Comparison of the current theories with the experimental results. The rolling speed is 46.23 m/s /9100 fpm and the lubricant temperature is 81°C /178°F, Mineral oil.

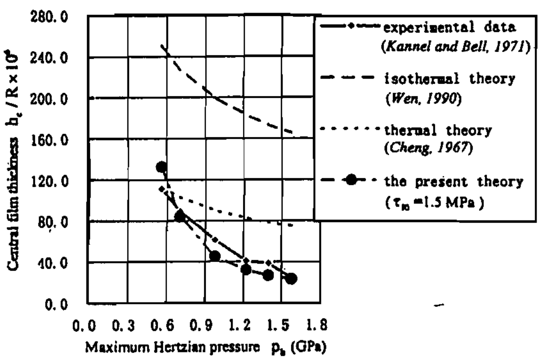

Fig. 9(b)—Comparison of the current theories with the experimental results. The rolling speed is 46.23 m/s /9100 fpm and the lubricant temperature is 81°C /178°F, polyphenyl ether (5P4E oil).

nesses in Figs. 9(a) and 9(b). Other theories are also compared. In the comparison, the ratio between the minimum and central film thickness in Kannel and Bell's experiment is assumed to be 0.75, and the thermal reduction factors of the central film thickness used by thermal theory are 0.6 and 0.45 for the mineral oil and the polyphenyl ether, respectively.

Figure 9 shows the conventional isothermal and thermal EHL theories much overestimate the film thickness but underestimate the film thickness sensitivity to heavy loads under high rolling speeds, while the present theory well matches the experimental film thickness.

THE CRITICAL RADIUS IN LINE CONTACT EHL FOR THE NON-CONTINUUM FILM REGIME

EHL film actually disappears under sufficiently heavy loads (Czichos and Kirschke,1972). EHL film failure stage transition is suspected to be gradual. In EHL, preceding film failure there may be a stage with an extremely thin film in part of the lubricated area with the thickness in molecular scale. The rheological behavior of this ultra thin film is different from the conventional ones and known as non-continuum-fluid (Tichy,1995).The lubricant film was identified as non-continuum when its thickness is lower than a critical value (Johnston et al., 1991). The present theory shows that around the Hertzian center of line contact EHL plays the non-continuum lubricant rheological behavior when:

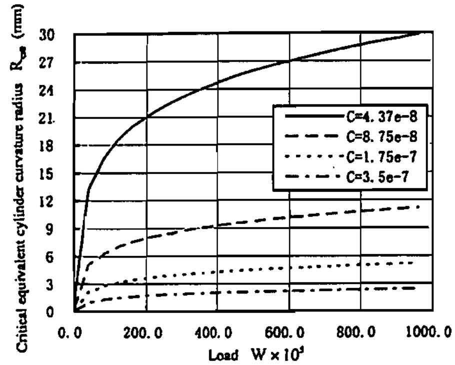

Fig. 10—The R_{cr0} values, G=4500.

$$H_{c,max}(W, C_p) \leq \frac{30nm}{R} \quad [20]$$

if 30nm is the critical film thickness of the non-continuum lubricant film. Equation [20] can be rewritten as :

$$R \leq \frac{30nm}{H_{c,max}(W, C_p)} \quad [21]$$

Define:

$$R_{cr0} = \frac{30nm}{H_{c,max}(W, C_p)} \quad [22]$$

Equation [21] predicts that the equivalent cylinder curvature radius (R) which is less than R_{cr0} generates the non-continuum lubricant film in line contact EHL. This manifests that when $R < R_{cr0}$, a mixture of the films in different rheological behaviors is produced in the whole elastohydrodynamic line contact, since the film in most of the inlet zone is understood as always continuum because of its thickness. For this case, conventional EHL analysis is incorrect. Figure 10 shows R_{cr0} for G = 4500, which is:

$$R_{cr0} = 8.716 \times 10^{-8} \frac{W^{0.2}}{(U_{b1} + \frac{K_1}{W^{n_i}})^{0.74}} mm \quad [23]$$

CONCLUSIONS

This paper investigates line contact EHL film thickness in isothermal and pure rolling conditions considering the limiting shear stress at the contact-lubricant interface. Based on the interfacial limiting shear stress, the EHL film thickness deviates from conventional predictions for comparatively high rolling speeds. The film thickness limit was found and the central film thickness limit was predicted.

Comparisons with the experimental results of Kannel and Bell support the present theory. The concept of the critical radius for the non-continuum lubricant film presence was proposed for line contact EHL. This concept shows that in line contact EHL, a mixture of the films in different rheological behaviors is produced in the whole lubricated area when the equivalent cylinder curvature radius is smaller than the critical one. This critical radius is determined by the load and the limiting shear stress at the interface. For this case, conventional EHL analysis is incorrect.

ACKNOWLEDGMENT

This research is funded by National Nature Science Foundation of P. R. China. Many thanks are expressed for this funding.

REFERENCES

(1) Bailey, M. W. and Cameron, A. (1973), " The Effects of Temperature and Metal Pairs On Scuffing," *ASLE Trans.*, **16**, p 121.

(2) Cheng, H. S. (1967), "Calculations of Elastohydrodynamic Film Thickness in High Speed Rolling and Sliding Contacts," Mechanical Technology, Inc. Technical Report, **MTI-67TR24**.

(3) Czichos, H. (1974), "Failure Modes of Sliding Lubricated Concentrated Contacts," *Wear*, **28**, pp 95-101.

(4) Czichos, H. and Kirschke, K. (1972), "Investigations Into Film Failure (Transition Point) of Lubricated Concentrated Contacts," *Wear*, **22**, pp 321-336.

(5) Ehret, P., et al. (1998), "On Lubricant Transport Conditions in Elastohydrodynamic Conjunctions," in *Proc. Roy. Soc. Lond.*, *A454*, pp 763-787.

(6) Johnson, K. L. and Tevaarwerk, J. L. (1977), "Shear Behavior of Elastohydrodynamic Oil Films," in *Proc. Roy. Soc. Lond.*, **356**, A, pp 215-236.

(7) Johnston, G. J., Wayte, R. and Spikes, H. A. (1991), " The Measurement and Study of Very Thin Lubricant Film in Concentrated Contacts," *Trib. Trans.*, **34**, pp 187-194.

(8) Kaneta, M., et al. (1996), "Abnormal Phenomena Appearing in EHL contacts," *ASME Jour. of Trib.*, **118**, pp 886-892.

(9) Kaneta, M., et al. (1992), "Effects of Elastic Moduli of Contact Surfaces in Elastohydrodynamic Lubrication," *ASME Jour. of Trib.*, **114**, pp 75-80.

(10) Kannel, J. W. and Bell, J. C. (1971), "Interpretations of the Thickness of Lubricant Films in Rolling Contact: Part I—Examination of Measurements Obtained by X-Rays," *ASME Jour. of Lubri. Tech.*, pp 478-484.

(11) Lee, D., Sanborn, D. M. and Winer, W. O. (1973), "Some Observations of the Relationship Between Film Thickness and Load in High Hertz Pressure Sliding Elastohydrodynamic Contacts," *ASME Jour. of Lubr. Tech.*, **95**, pp 386-390.

(12) Paul, G. R. and Cameron, A. (1979), "The Ultimate Shear Stress of Fluids at High Pressures Measured By a Modified Impact Microviscometer," in *Proc. Roy. Soc. Lond., A365*, pp 31-41.

(13) Rozeanu, L. (1980), "Slippage Phenomena At the Interface Between the Absorbed Layer and the Bulk of the Lubricant: Theory and Experiment," *Wear*, **64**, pp 245-257.

(14) Rozeanu, L. and Snarsky, L. (1978), "Effect of Solid Surface Lubricant Interaction on the Load Carrying Capacity of Sliding Bearings," *ASME Jour. of Lubr. Tech.*, **100**, pp 167-175.

(15) Tichy, J. A. (1995), "Modeling of Thin Film Lubrication," *Trib. Trans.*, **38**, pp 108-118.

(16) Wen, S. Z. and Yang, P. (1990), *Elastohydrodynamic Lubrication (in Chinese)*, Tsinghua Press, Beijing, P. R. of China.

(17) Wen, S. Z. and Zhang, Y. B. (2000), "EHL Performance of the Lubricant with Shear Strength: Part I-Boundary Slippage and Film Failure," *Trib. Trans.*, **43**, 4, pp 700-710.

(18) Yang, P., et al. (2001), "Formation of Steady Dimples in Point TEHL Contacts," *ASME Jour. of Trib.*, **123**, pp 42-49.

(19) Zhang, Y. B. and Wen, S. Z. (1998), "Prevention of Film Slippage in Isothermal Pure Rolling Line Contact EHL Under Heavy Load," *ASME Jour. of Trib.*, **1060 P/al.**

(20) Zhang, Y. B. and Wen, S. Z. (2002a), "An Analysis of Elastohydrodynamic Lubrication with Limiting Shear Stress: Part I-Theory and Solutions," *Trib. Trans.*, **45**, 2, pp 135-144.

(21) Zhang, Y. B. and Wen, S. Z. (2002b), "An Analysis of Elastohydrodynamic Lubrication with Limiting Shear Stress: Part II- Load Influence," *Trib. Trans.*, **45**, 2, pp 211-216.